PRAMANA — journal of physics

Vol. 80, No. 5
May 2013
pp. 785–796

Collapse revival behaviour of the entanglement between V-type three-level atoms and two-mode photons in nonlinear Jaynes–Cummings model

M MAHJOEI[1,2,*], M M GOLSHAN[2] and H SAFARI[3]

[1]Physics Department, Vali-Asr University, Rafsanjan, Iran
[2]Physics Department, Shiraz University, Pardis Eram, Shiraz, Iran
[3]Photonic Department, Kerman Graduate University of Technology, Mahan, Kerman, Iran
*Corresponding author. E-mail: mahjoei@vru.ac.ir

MS received 28 August 2012; revised 15 November 2012; accepted 10 December 2012

Abstract. In this paper the time evolution of von Neumann entropy, as a measure of entanglement between V-type three-level atoms and the union of a two-mode field, is studied. The atom–field interaction is assumed to occur in a Kerr-type medium with an intensity-dependent coupling. Introducing a Casmir operator whose eigenvalues, N, give total excitations in the system and commutes with the governing Hamiltonian, it is concluded that the latter is block-diagonal with ever growing dimensions. As we shall show, however, each block consists of two 2×2 blocks while all the others, $(N-1)$ in number, are 3×3. We then proceed to analytically calculate the time-evolution operator which is also block-diagonal, each block with the same properties as that of the Hamiltonian. Our calculations show that, as expected, the atom–field entanglement oscillates which, depending upon the initial state, exhibits the phenomenon of collapse revivals. It is further shown that collapse revivals occur whenever both 2×2 blocks are involved in the time evolution of the system. Properties of such behaviour in the entanglement are also discussed in detail.

Keywords. Atom–photon entanglement; nonlinear medium; von Neumann entropy; three-level atom; two-mode field.

PACS Nos 03.67.Bg; 03.67.Mn; 03.67.Hk; 42.50.Dv

1. Introduction

Generation of entanglement in multipartite quantum systems has been the subject of extensive theoretical and experimental studies regarding fundamental issues as well as its applications in quantum-information processing [1]. It is used in some protocols of quantum cryptography [2]. Superdense coding and quantum teleportation [3] are among the best-known applications of entanglement. The key element of many quantum communication protocols is formed by entangled photons which can easily be transported

through optical fibres or air. Therefore, they are ideal carriers of quantum information and are, e.g., used for entanglement-based quantum cryptography [4] or for the distribution of quantum information between remote locations [5–8]. On the other hand, trapped ions or neutral atoms are ideal resources for the reliable storage of quantum information. Together with the possibility to address and manipulate single qubits, they are a promising candidate for the realization of quantum memories or quantum computers [9–12]. The multipartite entangled states have recently attracted more attention in connection with multiparty communication protocols [13]. Amongst a variety of multipartite-multilevel systems, the entanglement of three-level atoms, qutrits, and multimode fields, inside a microwave cavity, has been proposed for application in quantum teleportation [14]. This growing interest, in particular, stems from new experimental reports on characterization, as well as control of multi-ions [15], multi-photons [16] or some thousand neutral atoms in the so-called cluster state [17] entanglement. In such systems, in spite of being multipartite, the elements are two-dimensional, forming multi-qubits [18]. However, as is well known, higher-dimensional systems offer advantages including large channel capacities in quantum communications with increased security [19] and even tests of quantum nonlocality [20]. However, a missing point in these scenarios is that the QED cavity may be filled with dielectrics which, under the influence of electromagnetic field, behave nonlinearly [21]. Therefore, the main aim of the present article is to investigate the effect of medium nonlinearities on the entanglement of a three-level (V-type) atom and a two-mode field inside a QED cavity. For future applications in quantum information sciences as, e.g., the quantum repeater [22,23] or quantum networks, the faithful mapping of quantum information between a stable quantum memory and a reliable quantum communication channel is essential. Because quantum states can in general not be copied, entanglement between the quantum memory and the communication channel is necessary. Therefore, entanglement between different species like atoms and photons is an essential resource. Combining the advantages of photons (information transport over large distances) and atoms (reliable information storage), atom–photon entanglement enables the interface between atomic quantum memories and photonic quantum communication channels and allows the distribution of quantum information over large distances.

The researches on entanglement mainly focus on handling two problems: How to generate an entanglement and how to make it long-lived. Recently, the interactions between the atom and the field are widely studied [24–28]. Compared to the two-level atom, the three-level atom has different transition characteristics. The quantum phenomena are more interesting for the three-level atom [29–31]. Therefore, it is necessary to deeply study the three-level atom. It is reasonable to generalize the Jaynes–Cummings (JC) model, the cornerstone for formulating the atom–field interaction, to include such nonlinear effects. To this end, the entanglement between a single-mode field and a three-level V-type atom [32], a two-mode field and a three-level Λ-type atom [33] or E-type atom [34] have been reported. Therefore, the aim of this paper is to present the influence of nonlinearities and, in particular, the initial states on the entanglement of three-level V-type atom and the union of two photonic modes.

In this work we first present the nonlinear Jaynes–Cummings Hamiltonian and introduce a Casimir operator that commutes with it. Consequently, it is shown that if the bases in the corresponding Hilbert space is numbered according to the eigenvalues of such a Casimir operator, the matrix representation of the total Hamiltonian as well as the

time-evolution operator are block-diagonal. Keeping this point in mind, the time evolution of the initial states, leading to the temporal behaviour of the von Neumann entropy, is easily determined. Inspecting the von Neumann entropy as a measure of entanglement between atom and union of photons, the roles of initial states and the nonlinearities are recognized.

This paper is organized as follows. In §2 we give a brief discussion of the von Neumann entropy as a measure of entanglement. In §3 the nonlinear Jaynes–Cummings Hamiltonian along with a Casimir operator are presented. We proceed to examine the matrix representation of the Hamiltonian and show that it is block-diagonal. We further demonstrate that each block consists of 2×2 and/or 3×3 subblocks which highly simplifies the calculation of eigenvalues and eigenvectors. In §4, atom–photon entanglement, as a function of time, along with the influence of different parameters on its behaviour, is given. Interpretation of the results and physical reasons are also discussed in this section. We highlight the more important aspects of the article in the concluding section.

2. Entanglement and von Neumann entropy

Entanglement is the quantum mechanical property that Schrödinger singled out many decades ago as 'the characteristic trait of quantum mechanics' and has been studied extensively in connection with Bell's inequality [35]. A pure state of a pair of quantum systems, A and B, is entangled if it is unfactorizable,

$$|\psi^{AB}\rangle \neq |\varphi^{A}\rangle \otimes |\chi^{B}\rangle, \tag{1}$$

while a mixed state is entangled if it cannot be represented as a mixture of factorizable pure states [36,37]. In fact, the entanglement related to a system containing subsystems, shows the joint information between the subsystems. That is, the degree of entanglement of a composite system is proportional to the nonlocal information in the system. Thus, by increasing the degree of entanglement, one would have less information about the subsystems.

For a combination of two subsystem, A and B (here the atomic and the union of photonic modes), in pure states, it has been well established that the von Neumann entropy,

$$S_{vN}(\rho_{AB}) = -\mathrm{Tr}[\rho_{AB} \log_2 \rho_{AB}], \tag{2}$$

where ρ_{AB}, the total density matrix, gives the number of qubits per state that can be stored in the combined system. It is evident that eq. (2) reduces to $-\Sigma_l \lambda_l \log_2 \lambda_l$, where λ_l are eigenvalues of ρ. On the other hand, the reduced von Neumann entropy, defined as,

$$E = S_{vN}(\rho_A) = S_{vN}(\rho_B) = -\mathrm{Tr}[\rho_A \log_2 \rho_A] = -\mathrm{Tr}[\rho_B \log_2 \rho_B], \tag{3}$$

where $\rho_{A(B)} = \mathrm{Tr}_{B(A)}(\rho_{AB})$, quantifies the number of qubits per state that can be stored in each subsystem. Alternatively, the reduced von Neumann entropy may be interpreted as the degree of entanglement between the subsystems. Evidently, if the subsystems are completely disentangled then $E = 0$ (i.e., full information about each subsystem is available), while for a complete entanglement $E = 1$ (information is evenly distributed among the subsystems). In what follows, we shall calculate the evolution of the degree of entanglement, given by eq. (3) for atomic states and photons.

3. The physical model and the time evolution operator

We consider a V-type atom with two upper levels, $|A\rangle$, $|B\rangle$, and one lower level, $|C\rangle$, interacting with a two-mode quantized electromagnetic field inside a cavity filled with a nonlinear medium. Denoting the atomic level frequencies by $\omega_A > \omega_B > \omega_C = 0$ and the photonic frequencies by Ω_A and Ω_B, the Hamiltonian of the system in the electric dipole and rotating-wave approximations can be written as

$$\mathbf{H} = \hbar \left(\sum_{i=A,B} \omega_i \boldsymbol{\sigma}_{ii} + \sum_{i=A,B} \Omega_i \mathbf{a}_i^\dagger \mathbf{a}_i + \chi_i \mathbf{a}_i^{\dagger 2} \mathbf{a}_i^2 + \sum_{i=A,B,\, j=A,B} g_i (\boldsymbol{\sigma}_{jC} f_i(\mathbf{a}_i^\dagger \mathbf{a}_i) \mathbf{a}_i + \text{h.c.}) \right), \tag{4}$$

where $\mathbf{a}_i(\mathbf{a}_i^\dagger)$ is the annihilation (creation) operator of the A, B modes and σ_{ij}, $i, j = A, B, C$, with commutation relations $[\sigma_{ij}, \sigma_{kl}] = \sigma_{il}\delta_{jk} - \sigma_{kj}\delta_{il}$, represents the atomic operators. Moreover, in eq. (4) the strength of Kerr nonlinearity is given by χ_i while the intensity-dependent couplings $g_i f_i(\mathbf{a}_i^\dagger \mathbf{a}_i)$ arise from the commutation relations of the deformed oscillators inside the nonlinear dielectric [38,39].

A Casimir operator of the present atom–field system reads as

$$\mathbf{N} = \sum_{i=A,B} \mathbf{a}_i^\dagger \mathbf{a}_i + |i\rangle\langle i| \equiv \mathbf{N}_A + \mathbf{N}_B, \tag{5}$$

where

$$\mathbf{N}_A = \mathbf{a}_A^\dagger \mathbf{a}_A + |A\rangle\langle A| \qquad \text{and} \qquad \mathbf{N}_B = \mathbf{a}_B^\dagger \mathbf{a}_B + |B\rangle\langle B|.$$

It may easily be shown that $\mathbf{N}$ commutes with $\mathbf{H}$ of eq. (4). The eigenvalues of operator $\mathbf{N}$; N, gives the total excitations present in the combined atom–field system. The total Hilbert space is the direct product of the first, second field modes, $\mathcal{H}_{F_A}, \mathcal{H}_{F_B}$, respectively, and atomic Hilbert subspaces:

$$\mathcal{H} = \mathcal{H}_{F_A} \otimes \mathcal{H}_{F_B} \otimes \mathcal{H}_{\text{Atom}}. \tag{6}$$

The identity in the total Hilbert space, reads as

$$\sum_{n_A, n_B, j=A,B,C} |n_A, n_B, j\rangle\langle n_A, n_B, j|. \tag{7}$$

Consequently, the matrix representation of eq. (4) is block-diagonal with respect to the eigenstates of $\mathbf{N}$. In what follows, it is verified that each block is a $(3N + 1) \times (3N + 1)$ matrix, consisting of two 2×2 block matrices while the remaining N–1 ones are 3×3. As a result, the time-evolution matrix is also block-diagonal, again with two 2×2 block matrices and N–1 blocks of dimensions 3. For a fixed number of excitations, N, the bases are of the form, $|N - N_B, N_B, C\rangle$, $|N - N_B - 1, N_B, A\rangle$ and $|N - N_B, N_B - 1, B\rangle$ (or equally, $|N_A, N - N_A, C\rangle$, $|N_A - 1, N - N_A, A\rangle$ and $|N_A, N - N_A - 1, B\rangle$), where $0 \leq N_B(N_A) \leq N$. Disregarding the unphysical states with negative values of excitations, it is seen that for $N_B = 0$ (or N), states of the type $|N, 0, C\rangle$ and $|N - 1, 0, A\rangle$ ($|0, N, C\rangle$ and

$|0, N-1, B\rangle$) give the 2×2 blocks. On the other hand, for any other values of N_A (or N_B) the three corresponding states contribute, giving 3×3 blocks. It is then seen that each block corresponding to the fixed value of excitation is of dimensions $2 \times 2 + 3 \times (n-1) = 3N + 1$. The foregoing discussions imply that, depending on the excitation presented in the initial state, only 2×2 and/or 3×3 blocks determine the evolution of the system. In the remaining part of this section this procedure is used to present the matrix elements of 2×2 subblocks.

For no excitations, $N = 0$, the system is described by the state $|0_A, 0_B, C\rangle$ which is separable and stationary. For $\mathbf{N} \geq 1$, on the other hand, the relevant bases ('bare states') are:

$$|1\rangle \equiv |N, 0, C\rangle\,, \qquad |2\rangle \equiv |N-1, 0, A\rangle\,, \qquad |3\rangle \equiv |0, N, C\rangle\,,$$
$$|4\rangle \equiv |0, N-1, B\rangle\,, \qquad N \geq 1. \tag{8}$$

The corresponding matrix representation of $\mathbf{H}$ is then 4×4 with two 2×2 subblocks, belonging to channels of excitations, as specified in eq. (5). Diagonalizing this matrix gives the 'dressed states' as

$$\varphi_A = \begin{pmatrix} \dfrac{\Delta_A \pm \alpha_A}{\sqrt{2\alpha_A(\alpha_A \mp \Delta_A)}} \\ \dfrac{2g_A\sqrt{N} f_A\,(N-1)}{\sqrt{2\alpha_A(\alpha_A \mp \Delta_A)}} \\ 0 \\ 0 \end{pmatrix} \tag{9}$$

and

$$\varphi_B = \begin{pmatrix} 0 \\ 0 \\ \dfrac{\Delta_B \pm \alpha_B}{\sqrt{2\alpha_B(\alpha_B \mp \Delta_B)}} \\ \dfrac{2g_B\sqrt{N} f_B(N-1)}{\sqrt{2\alpha_B(\alpha_B \mp \Delta_B)}} \end{pmatrix} \tag{10}$$

with eigenenergies,

$$E_{A(B)} = \frac{\hbar}{2}\left(\xi_{A(B)} \pm \alpha_{A(B)}\right). \tag{11}$$

In eqs (9) through (11), Rabbi oscillations for each channel (but not a combination of the two) occur at frequencies,

$$\alpha_{A(B)} = \sqrt{\Delta^2_{A(B)} + 4g^2_{A(B)} N f^2_{A(B)}(N-1)}, \tag{12}$$

where the modified detuning is $\Delta_{A(B)} = [1 + 2\,(N-1)\chi_{A(B)}]\Omega_{A(B)} - \omega_{A(B)}$. As seen below, the part $\xi_{A(B)} = [2N - 1 + 2\,(N-1)^2\chi_{A(B)}]\Omega_{A(B)} + \omega_{A(B)}$ in eq. (11) gives rise

to envelopes (collapse-revivals) on the oscillations when both channels are open in the initial state but drops out otherwise. It is noted that for one excitation, the Kerr parameter $\chi_{A(B)}$ does not contribute. In the 'dressed' representation the elements of time-evolution matrix are $U_{ii}^{\text{dressed}} = \mathrm{e}^{-iE_it/\hbar}$, where E_i are given in eq. (11). The elements of U in the 'bare' representation, which are obtained by the transformation $U^{\text{bare}} = V^{\dagger}U^{\text{dressed}}V$, with the transformation matrix V constructed from the dressed states in eqs (9) and (10), then reads as

$$\begin{aligned}
\left(U_{11}^{\text{bare}}\right)_{A(B)} &= \mathrm{e}^{-(i/2)\xi_{A(B)}t}\left[\cos\left(\frac{\alpha_{A(B)}}{2}t\right) - i\left(\frac{\Delta_{A(B)}}{\alpha_{A(B)}}\right)\sin\left(\frac{\alpha_{A(B)}}{2}t\right)\right]\\
\left(U_{22}^{\text{bare}}\right)_{A(B)} &= \mathrm{e}^{-(i/2)\xi_{A(B)}t}\left[\cos\left(\frac{\alpha_{A(B)}}{2}t\right) + i\left(\frac{\Delta_{A(B)}}{\alpha_{A(B)}}\right)\sin\left(\frac{\alpha_{A(B)}}{2}t\right)\right]\\
\left(U_{12}^{\text{bare}}\right)_{A(B)} &= \left(U_{21}^{\text{bare}}\right)_{A(B)} = \mathrm{e}^{-(i/2)\xi_{A(B)}t}\,\frac{2ig_{A(B)}\sqrt{N}\,f_{A(B)}\,(N-1)}{\alpha_{A(B)}}\sin\left(\frac{\alpha_{A(B)}}{2}t\right).
\end{aligned} \tag{13}$$

Similarly, the elements of 3×3 subblocks of the time-evolution matrix, arising from higher excitations, may also be derived. However, the resulting expressions are so lengthy that, for the sake of brevity, we do not present them here. Nonetheless, it is clear that, at least in principle, time evolution of the system of V-type atoms and two-mode fields can be determined analytically.

In the next section we employ the time-evolution matrix so obtained to investigate the dynamics of entanglement between the atomic states and the union of two-mode photons for some specific examples. The examples, however, serve to exhibit the general dynamical behaviour of the phenomenon of collapse-revival in the entanglement.

4. Results and discussions

In the previous section we have demonstrated how the time-evolution matrix for the system of V-type three-level atoms and two-mode electromagnetic fields may be calculated. We have also shown how the calculation of 2×2 blocks may be extended to include any number of excitations in the system. In this section we try to study, qualitatively, the dependence of the collapse-revival behaviour of the entanglement on the initial conditions as well as the atom–field coupling, with the help of numerical calculations. To this end, we investigate the dynamics of entanglement in three different cases where the initial state is (i) a linear combination of system bases in which the atom is in its ground state, (ii) a linear combination of system bases, each belonging to one of the 2×2 subblocks with the atom being in state A or B and (iii) a linear combination of all system bases constructing the 2×2 subblocks. In the calculations the required parameters are chosen as follows: $\omega_A = 1$ (scaled), $\omega_B = 0.93$, $\Omega_i = (9/10)\omega_i$, $g_i = 0.15\Omega_i$, $\chi_i = 0.9\Omega_i$.

Let us first consider the case, $N=1$, with the corresponding numerical results depicted in figure 1. In this figure various linear combinations of system bases with equal weights, (figures 1a–1c), and also with different weights (figures 1d–1f), are considered as the initial state of the system. This figure is produced using an intensity-dependent coupling of the form $f(\mathbf{a}_i^{\dagger}\mathbf{a}_i) = (1 + \mathbf{a}_i^{\dagger}\mathbf{a}_i)^{-1/2}$. From figure 1 we note that the time evolution

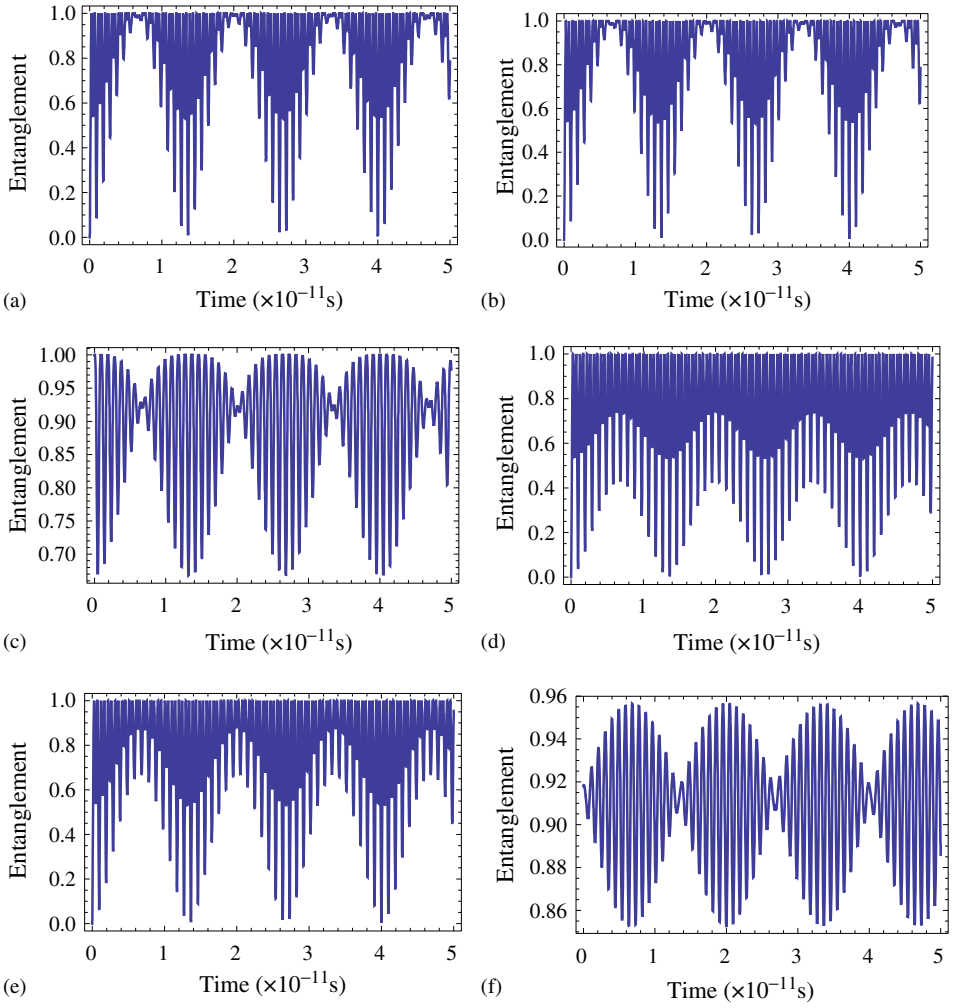

Figure 1. Time evolution of the entanglement for $N=1$. (**a**) $\frac{1}{\sqrt{2}}(|1,0,C\rangle+|0,1,C\rangle)$, (**b**) $\frac{1}{\sqrt{2}}(|0,0,A\rangle+|0,0,B\rangle)$, (**c**) $\frac{1}{\sqrt{4}}(|1,0,C\rangle+|0,0,A\rangle+|1,0,C\rangle+|0,0,B\rangle)$ (initial state $\varphi(0)$ is considered), (**d**) $\frac{1}{\sqrt{10}}(|1,0,C\rangle+3\,|0,1,C\rangle)$, (**e**) $\frac{1}{\sqrt{20}}(2\,|0,0,A\rangle+4\,|0,0,B\rangle)$ and (**f**) $\frac{1}{\sqrt{30}}(|1,0,C\rangle+2\,|0,0,A\rangle+3\,|0,1,C\rangle+4\,|0,0,B\rangle)$ ($\varphi(0)$ is constructed from the bases with different weights).

of entanglement is, as expected, an oscillatory one. However, the oscillations follow the patterns of collapse revivals, whose frequency is independent of the choice of initial states. Moreover, the maximum value of atom–field entanglement is one instead of log 3, which is a characteristic of three-level atoms. This is due to the fact that for the initial conditions used in this figure the atom is either in the ground state with photons of a particular mode present or the atom is excited with no photon present. This situation is identical to the system of two-level atom and one photonic mode, with maximal entanglement of one. It

is further noticed that the patterns of collapse revival are more distinct when all atomic states are present in the initial state.

To investigate the temporal behaviour of atom–field entanglement for larger values of excitation, N, in figure 2, it is illustrated for the initial state:

$$\psi(0) = \frac{1}{\sqrt{4}}\left(|4, 0, C\rangle + |3, 1, C\rangle + |2, 2, C\rangle + |1, 3, C\rangle + |0, 4, C\rangle\right)$$

with total excitations of 4.

The intensity-dependent coupling in this figure are $f_1(\mathbf{a}_i^\dagger \mathbf{a}_i) = (1 + \mathbf{a}_i^\dagger \mathbf{a}_i)^{-1/2}$, $f_2(\mathbf{a}_i^\dagger \mathbf{a}_i) = 1$ and $f_3(\mathbf{a}_i^\dagger \mathbf{a}_i) = (1 + \mathbf{a}_i^\dagger \mathbf{a}_i)^{+1/2}$, from figures 2a to 2c, respectively. It is noted from figure 2 that the atom–field entanglement is the largest for f_3 and the least entanglement occurs for f_1. This result is expected because the stronger the atom–field coupling, more and more states get involved which, in turn, yields a larger entanglement.

We further advance our study by considering initial states which contain states of different excitations, namely, photonic coherent states. Specifically we take the photonic coherent states as

$$|\eta\rangle = |\alpha, M\rangle = \sum_{0}^{M} \frac{|\alpha|^n}{\sqrt{n!}} \mathrm{e}^{-|\alpha|^2/2} |n\rangle,$$

with $|\alpha|^2$ giving the mean number of photons. Although a coherent state is in fact defined as the summation runs to infinity, our numerical calculations indicate that the summation

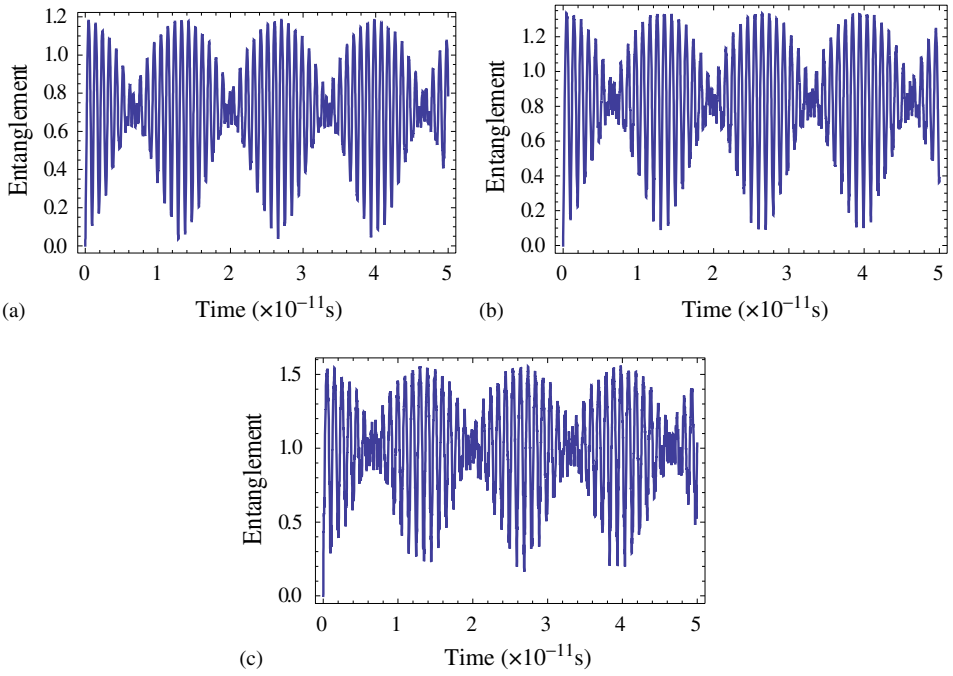

Figure 2. Time evolution of entanglement for $N = 4$ with the atom–field coupling $f(n)$ being (**a**) $1/\sqrt{n+1}$, (**b**) 1 and (**c**) $\sqrt{n+1}$.

may be truncated at $M = 16$, giving rise to a 425×425 matrix representations. This cut-off introduces an error of less than %0.1 which is indeed negligible. The initial state is then taken as $|\eta_A, \eta_B, C\rangle$, for a coupling of $(n+1)^{-1/2}$. Figure 3 shows the time evolution of entanglement for the case in hand. In this figure the initial mean photon numbers vary from figures 3a to 3c and figures 3a, 3b and 3c correspond to $\alpha_A = \alpha_B = 1$, $\alpha_A = \alpha_B = 2\sqrt{2}$ and $\alpha_A = \alpha_B = 4$, respectively. From figure 3 it is observed that as the photonic mean number, $|\alpha|^2$, tends to $M/2$ the collapse revival pattern is more pronounced with a greater time-averaged value. The reason behind this behaviour is the fact that the defining series more accurately resembles a real coherent distribution when it is terminated at twice the photonic mean.

Finally, in figure 4 the effect of nonlinear parameters, χ_i, on the entanglement, also for coherent distributions, is illustrated. The graphs in this figure correspond to $\chi_i = 0.2\Omega_i$ (figure 4a), $\chi_i = 0.5\Omega_i$ (figure 4b), $\chi_i = 0.9\Omega_i$ (figure 4c), with $f(n) = (n+1)^{-1/2}$. As can be seen from this figure, the pattern is more distinct for larger value of χ_i while the time-averaged entanglement is reduced. The physical reason for this conclusion is that as χ_i increases the energy spacing of the bases also increases and it is harder for a fixed coupling to couple different states.

In figure 4 the effect of nonlinearity of the medium, χ, on the entanglement is explored. The graphs correspond, from figures 4a to 4c, to $\chi_i = 0.2\Omega_i$, $0.5\Omega_i$ and $0.9\Omega_i$ with $f_i(n_i) = 1/\sqrt{n_i + 1}$. As can be readily seen the collapse-revival pattern is more pronounced as χ increases.

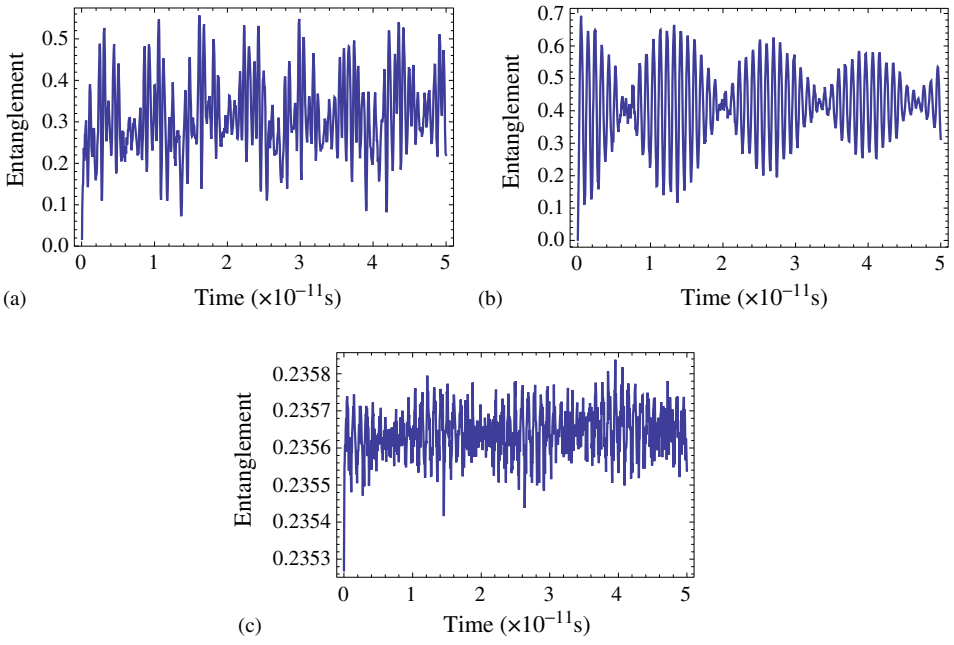

Figure 3. Time evolution of entanglement for photonic coherent distributions with $M = 16$. (**a**) $\alpha = 1$, (**b**) $\alpha = 2\sqrt{2}$ and (**c**) $\alpha = 4$.

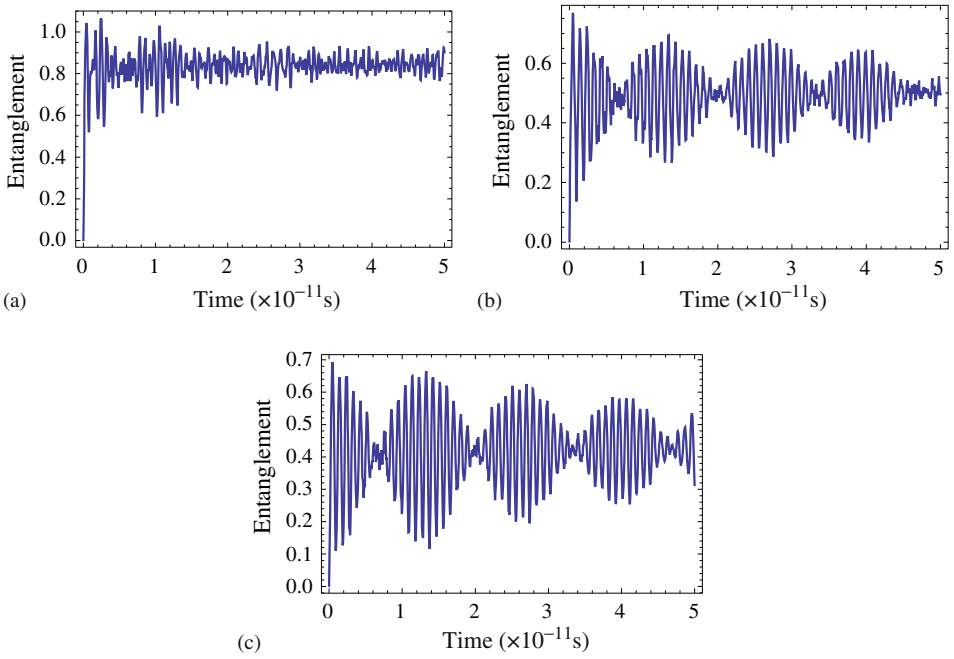

Figure 4. Time evolution of entanglement for photonic coherent distributions with $M = 16$. (**a**) $\chi_i = 0.2\Omega_i$, (**b**) $\chi_i = 0.5\Omega_i$ and (**c**) $\chi_i = 0.9\Omega_i$.

5. Conclusion

We employ the von Neumann entropy as a measure of entanglement and consider its evolution. Introducing a Casimir operator, we have demonstrated that the systems in Hamiltonian, as well as the density matrix, are block-diagonal. This point, in turn, enables us to compute the required eigenvalues more effectively. The procedure is then used to investigate the effects of initial number of excitations, Kerr-type parameters and the intensity-dependent couplings on the temporal behaviour of the entanglement. Although the results are thoroughly discussed in §4, in what follows we outline the more important aspects of this work.

- The atom–photon entanglement exhibits the pattern of collapse revival. The pattern is more distinct for initial states of higher excitations and/or weights of the bases involved (see figures 1–4).
- Where the initial state involves photonic coherent distributions of the type $|\alpha, M\rangle = \sum_0^M \frac{|\alpha|^n}{\sqrt{n!}} e^{-|\alpha|^2/2} |n\rangle$, the time-averaged entanglement is enhanced whenever the photonic mean number coincides with $M/2$ (see figures 3 and 4).
- Stronger atom–field couplings (here couplings of the form $\sqrt{n+1}$) lead to the enhancement of entanglement. The time-averaged entanglement also increases (see figure 2).

- As the nonlinear Kerr parameters are increased the degree of entanglement decreases both in magnitude and time average (see figure 4).

Acknowledgements

This work has been partly supported by a grant from the Research Council of Shiraz University, under the contract 90-GR-SC-82.

References

[1] L Lamata, J Leon, D Salgado and E Solano, *Phys. Rev. A* **74**, 052336 (2006)
[2] T Jennewein, C Simon, G Weihs, H Weinfurter and A Zeilinger, *Phys. Rev. Lett.* **84**, 4729 (2000)
[3] L Ye and G Guo, *Phy. Rev. A* **71**, 034304 (2005)
[4] A Ekert, *Phys. Rev. Lett.* **67**, 661 (1991)
[5] C H Bennett, G Brassard, C Crepeau, R Jozsa, A Peres and W K Wootters, *Phys. Rev. Lett.* **70**, 1895 (1993)
[6] D Bouwmeester, J W Pan, K Mattle, M Eibl, H Weinfurterm and A Zeilinger, *Nature* **390**, 575 (1997)
[7] J W Pan, D Bouwmeester, H Weinfurter and A Zeilinger, *Phys. Rev. Lett.* **80**, 3891 (1998)
[8] K Mattle, H Weinfurter, P G Kwiat and A Zeilinger, *Phys. Rev. Lett.* **76**, 4656 (1996)
[9] C F Roos, M Riebe, H Haner, W Hansel, J Benhelm, G P T Lancaster, C Becher, F Schmidt-Kaler and R Blatt, *Science* **304**, 1478 (2004)
[10] J Chiaverini, J Britton, D Leibfried, E Knill, M D Barrett, R B Blakestad, W M Itano, J D Jost, C Lange, R Ozeri, T Schaetz and D J Wineland, *Science* **308**, 997 (2005)
[11] D Schrader, I Dotsenko, M Khudaverdyan, Y Miroshnychenko, A Rauschenbeutel and D Meschede, *Phys. Rev. Lett.* **93**, 1501 (2004)
[12] R Raussendorf and H J Briegel, *Phys. Rev. Lett.* **86**, 5180 (2001)
[13] I Chuang and M Nielsen, *Quantum computation and quantum information* (Cambridge University Press, Cambridge, 2000)
[14] C H Bennett, G Brassard, C Crepeau, R Jozsa, A Peres and W K Wootters, *Phys. Rev. Lett.* **70**, 1895 (1993)
[15] R G Hafner, W Hansel, C F Roos, J Benhelm, D Chek-al-kar, M Chwalla, T Korber, U D Rapol, M Riebe, P O Schmidt, C Becher, O Guhne, W Dur and R Blatt, *Nature* **438**, 643 (2005)
[16] Z Zhao, Y A Chen, A N Zhang, T Yang, H J Briegel and J W Pan, *Nature* **430**, 54 (2004)
[17] M Greiner, O Mandel, T Esslinger, T W Hansch and I Bloch, *Nature* **415**, 39 (2002)
[18] P Aniello, C Lupo, M Napolitano and M G A Paris, *Eur. J. Phys. D* **41**, 579 (2007)
[19] P B Dixon, G A Howland, J Schneeloch and C Howell, *Phys. Rev. Lett.* **108**, 14 (2012)
[20] R Garcia-Patron, J Fiurasek and N J Cerf, *Quantum information with continuous variables of atoms and light* (Imperial College Press, London, 2007)
[21] S Goto, A C Hale, R W Tucker and T J Walton, *Phys. Rev. A* **85**, 034103 (2012)
[22] H J Briegel, W Dur, J I Cirac and P Zoller, *Phys. Rev. Lett.* **81**, 5932 (1998)
[23] W Dur, H J Briegel, J I Cirac and P Zoller, *Phys. Rev. A* **59**, 169 (1999)
[24] S J D Phoenix and P L Knight, *Phys. Rev. A* **44**, 6023 (1991)
[25] S J D Phoenix and P L Knight, *Phys. Rev. Lett.* **66**, 2833 (1991)

[26] A J Wonderen, F Motamed and K Lendi, *J. Phys. A: Math. Gen*. **31**, 3395 (1995)
[27] M F Fang and H E Liu, *Phys. Lett*. **200**, 250 (1995)
[28] J Gea-Banacloche, *Phys. Rev. A* **44**, 5913 (1990)
[29] H I Yoo and J H Eberly, *Phys. Rep*. **118**, 239 (1985)
[30] D T Pegg, R Loudon and P L Knight, *Phys. Rev. A* **33**, 4085 (1986)
[31] M Schubert, I Siemers, R Blatt, W Neuhauser and P E Toschek, *Phys. Rev. Lett*. **68**, 3016 (1992)
[32] A S F Obada, A A Eied and G M Abd Al-Kader, *Int. J. Theor. Phys*. **48**, 380 (2009)
[33] A S F Obada, A A Eied G M Abd Al-Kader, *J. Phys. B: At. Mol. Opt. Phys*. **41**, 195 (2008)
[34] A S F Obada and A A Eied, *Opt. Commun*. **282**, 2184 (2009)
[35] R F Werner and M M Wolf, *Phys. Rev. A* **64**, 032112 (2001)
[36] M J Donald, M Horodecki and O Rudolph, *J. Math. Phys*. **43**, 4252 (2002)
[37] C H Bennett, D P DiVincenzo, J A Smolin and W K Wootters, *Phys. Rev. A* **54**, 3824 (1996)
[38] J Crnugelj, M Martinis and V Mikuta-Martinis, *Phys. Rev. A* **50**, 3545 (1994)
[39] Z Chang, *Phys. Rev. A* **47**, 5017 (1993)